Front. Electr. Electron. Eng. China 2007, 2(3): 338–344
DOI 10.1007/s11460-007-0064-1

RESEARCH ARTICLE

XIE Chenbo, ZHOU Jun, YUE Guming, QI Fudi, FAN Aiyuan

New mobile Raman lidar for measurement of tropospheric water vapor

Abstract The content of water vapor in atmosphere is very little and the ratio of volume of moisture to air is about 0.1%–3%, but water vapor is the most active molecule in atmosphere. There are many absorption bands in infrared (IR) wavelength for water vapor, and water vapor is also an important factor in cloud formation and precipitation, therefore it takes a significant position in the global radiation budget and climatic changes. Because of the advantages of the high resolution, wide range, and highly automatic operation, the Raman lidar has become a new-style and useful tool to measure water vapor. In this paper, first, the new mobile Raman lidar's structure and specifications were introduced. Second, the process method of lidar data was described. Finally, the practical and comparative experiments were made over Hefei City in China. The results of measurement show that this lidar has the ability to gain profiles of ratio of water vapor mixing ratio from surface to a height of about 8 km at night. Meanwhile, the measurement of water vapor in daytime has been taken, and the profiles of water vapor mixing ratio at ground level have been detected.

Keywords optics, lidar, water vapor, aerosol, Raman

1 Introduction

Water vapor, also aqueous vapor, is the gas phase of water. In the Earth, water vapor is one state of the water cycle within the hydrosphere, and it is replenished by evaporation from the seas, lakes, rivers, the transpiration of plants, as well as other biological and geological processes. Water vapor represents a small but environmentally significant constituent of the atmosphere. Besides accounting for most of the Earth's natural greenhouse effect, which warms the planet, water vapor also condenses to form clouds, which may act to warm or cool, depending on the circumstances. In general terms, atmospheric water strongly influences and is strongly influenced by weather, and weather is modified by climate [1]. On the other hand, water vapor has many absorption bands in infrared wavelengths. It absorbs this infrared wavelength and re-radiates it in all directions including back to Earth. It makes water vapor become an important factor in solar-earth radiation budget. Thus, increased knowledge of water vapor concentration and motion can lead to a better understanding of cloud formation, convective storm development, and the hydrological cycle [2].

Optical remote sensing technology is a new and useful tool in the research of atmospheric observation [3–5], and lidar (light detection and range) is its crucial component [6–9]. As one kind of lidar, Raman lidar system is designed specially to detect Raman wavelength-shifted light from molecules in the atmosphere, and to measure the content of these molecules. The early work of Melfi [10] and Cooney et al [11] in the late 1960s demonstrated the technique of Raman spectroscopy in the measurement of tropospheric water vapor. Later, with the development in laser, optical filter, and signal detecting technology, the ability of Raman lidar for measuring water vapor was improved greatly. Compared with the common observation facilities, lidar has the ability to continuously take measurements with higher spatial and temporal resolution. In situ measurements from airplanes or balloons are very costly and cannot provide data at low and high altitudes simultaneously. The latter advantage is also applied to measurements with radiosondes. Passive methods using radiation from the sun (or moon) lack the required height resolution. So, as a new type and important tool to probe atmospheric water vapor, Raman lidar has been applied widely in meteorological, climatic, radiant, and environmental researches [12–14].

To improve the range of measurement and motility of lidar, the first mobile Raman-Mie scattering lidar system (RML lidar) has been developed by Anhui Institute of Optics and Fine Mechanics (AIOFM), Chinese Academy of Sciences, in October 2004. It was used for measuring horizontal

Translated from *Acta Optica Sinica*, 2006, 26(9): 1 281–1 286 [译自: 光学学报]

XIE Chenbo (✉), ZHOU Jun, YUE Guming, QI Fudi, FAN Aiyuan
Center for Atmospheric Optics, Anhui Institute of Optics and Fine Mechanics, Chinese Academy of Sciences, Hefei 230031, China
E-mail: cbxie@aiofm.ac.cn

visibility [15], tropospheric aerosol, and water vapor. This paper only describes the part of water vapor measurement using RML lidar. Initially, the RML lidar equipment is detailed, the method of derivation is then given, and the typically observed results of water vapor over Hefei and their analysis are presented finally.

2 Equipment of RML lidar

Raman scattering is a weak molecular-scattering process that is characterized by a shift in wavelength of the scattered beam of light relative to the incident one. The amount of this shift depends on the rotational-vibrational energy level structure of the particular molecule being considered and is unique to it. Therefore, for a photon of certain incident wavelength, the shifted wavelength of the scattered photon is a signature of the molecule doing the scattering. This is the type of Raman scattering that is used in the present experiment. The RML lidar is on the basis of a double and triple frequency Nd: YAG laser transmitter, an optical telescope receiver, and various signal-processing and data-acquisition electronics. The pulsed laser beam is directed vertically through the atmosphere. As the laser beam propagates in air, it interacts with water molecule and nitrogen molecule. The backscattered radiation caused by Raman processes is detected and recorded as a function of height. These return signals are analyzed to determine the water vapor mixing ratio. To enable greater mobility, the whole RML lidar system (requiring only external electrical power) is housed in a climate-controlled 6.5 m mobile trailer, and is fully computer automated. Its structure and specifications are given in Fig. 1 and Table 1 respectively.

The laser of RML lidar is a continuum 8020 Nd: YAG that is operated in the triple frequency mode with an output wavelength of 355 nm, and the energy is 300 mJ with a repetition rate of 20 Hz and divergence less than 0.45 mrad. The transmitter optics of RML lidar includes two paths. In one path, after being expanded three-fold, the pulse laser beam with 85% energy is directed upward into the atmosphere for the "long range" water vapor measurement. In another path, the residual laser is transmitted vertically into the atmosphere by reflector installed at the pitch axis of the telescope. This laser acts as the radiation source for measurement of the "short range" water vapor.

The telescope used in RML lidar is 0.4 m, f/10 Cassegrain design with a variable field stop (Iris-1) is adjustable from 0.5 to 3 mrad field of view. All reflective surfaces of the telescope are plated with ultra-high transmission coating, so that the maximum reflection is within the range of 300–550 nm. Both the lights at 386.7 nm and 407.8 nm produced by Raman backscatter from nitrogen and water vapor are reflected into the unit of water vapor measurement by the beamsplitter 1 (BS-1). The baffler installed in telescope and variable field stop are used to limit the field of view of lidar system, and to

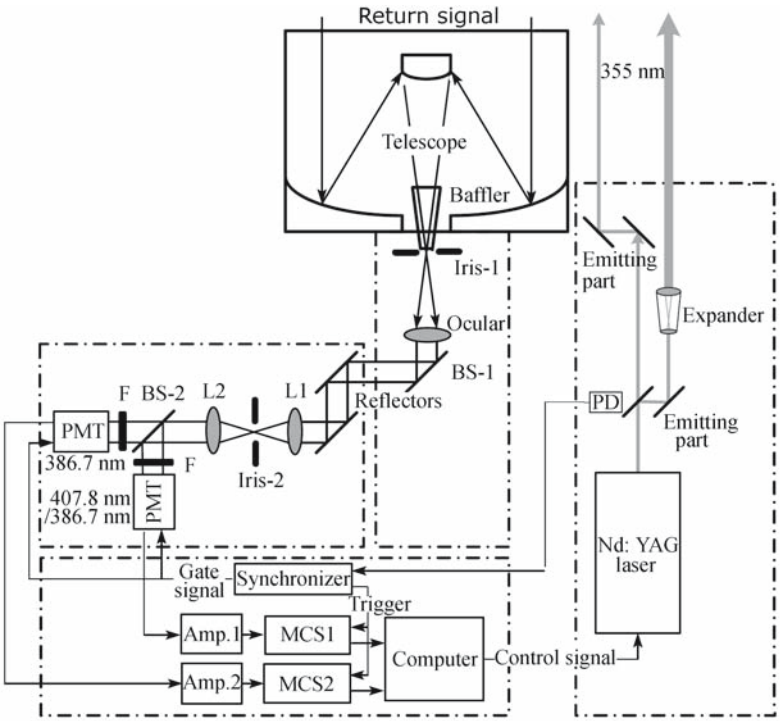

PD: photo diode, L: lens, F: filter, BS: beamsplitter

Fig. 1 Schematic diagram of RML lidar system

Table 1 Specification of RML lidar system

Transmitter optics		Receiver optics		Data acquisition and control	
Laser: Nd: YAG type (continuum powerlite 8020)		Telescope: cassegrain type (Meade Lx200 GPS)		PMT: EMI9813B × 2	
Wavelength /nm	355	Diameter /m	0.4	Quantum efficiency /%	> 25
Pulse energy /mJ	300	Focal length /m	4	Amplifier: VT120B × 2	
Stability %	± 4.0	Field of view /mrad	0.5–3	Gain	200
PRF/Hz	20	Filter: Barr Inc.		Bandwidth /MHz	350
Divergence/mrad	< 0.45	Bandwidth /nm	4.5@386.7 & 407.8	Data acquisition: MCS-pci × 2	
Pulse width /ns	6–8	Transmission%	> 30@386.7 & 407.8	Sample rate /MHz	150
Expander	× 3			Resolution /ns	200
				PC: WS-855	

decrease the background light scattered from the sky in daytime measurement. Two Raman scattered lights in the water vapor unit first pass through the beamsplitter group and lens, then are separated into two pieces by beamsplitter 2 (BS-2), with 12% of the light of at 386.7 nm and the whole at 407.8 nm directed into the water channel, and 88% of the light at 386.7 nm into the nitrogen channel. The light at 386.7 nm in water channel is just to correct optical alignment difference between two Raman channels in "short range" measurement. In each set of channels, through the corresponding interference filter and attenuators, the light is detected by the photomultiplier tube (PMT) finally. Both the mirrors in the beam splitter group are plated with the special coating to make them only reflect the lights at wavelengths of 386.7 nm and 407.8 nm, and permeate the other scattered lights for restricting background radiation within the lowest limits. Beside the alignment of transmitter and receiver optic axes, the work of Iris-2, and lens of L1 and L2 is to confine the received lights in detecting channels, especially for the lights in "short range".

Because the Raman scattering light is very weak, the photon counting technology is used in the data acquisition of RML lidar. Because of the larger dynamic of return signal, the PMT with active gate circuit was used to detect the returned signal in the "long range" (> 1–2 km) and the same PMT with an inactive one in "short range" (< 3 km) at different times. Finally, the whole signal is obtained by gluing these two signals through the region where both signals are valid and have a high signal to noise ratio.

3 Method

The backscattered signals from Raman water vapor channel at 407.8 nm and from Raman nitrogen channel at 386.7 nm are given by the following equations respectively [14]

$$S_{\mathrm{H}}(z)=\frac{k_{\mathrm{H}}}{z^2}\sigma_{\mathrm{H}}(\pi)n_{\mathrm{H}}(z)q(\lambda_0,z_0,z)q(\lambda_{\mathrm{H}},z_0,z) \tag{1}$$

$$S_{\mathrm{N}}(z)=\frac{k_{\mathrm{N}}}{z^2}\sigma_{\mathrm{N}}(\pi)n_{\mathrm{N}}(z)q(\lambda_0,z_0,z)q(\lambda_{\mathrm{N}},z_0,z) \tag{2}$$

where $s_x(z)$ is the return signal caused by channel x; λ_x is the wavelength of corresponding light caused by channel x; λ_o refers to the output laser wavelength (355 nm); k_x is the proportionality constant for channel x that accounts for the system optical efficiency, the telescope receiver area, the photomultiplier tube spectral efficiency, and the laser output energy; $\sigma_x(\pi)$ is the backscatter cross section for species x caused by Raman scattering; $n_x(z)$ is the number density for species x as a function of height z; $q(\lambda_x, z_o, z)$ is the atmospheric transmissivity from the lidar at height z_0 to height z at wavelength λ_x and equal to

$$\exp\left(-\int_{z_0}^{z}\alpha_{\lambda_x}(z')\,\mathrm{d}z'\right)$$

Here, $a_{\lambda x}$ is the volume extinction coefficient at wavelength λ_x.

The subscript x represents H, which refers to the Raman water vapor parameters, or N, which refers to the Raman nitrogen parameters.

According to the definition of water vapor mixing ratio, it is the mass of water vapor M_{H} divided by the mass of dry air M_{dry} in a given volume. As a function of height the water vapor mixing ratio can be expressed as

$$w(z)=\frac{n_{\mathrm{H}}(z)}{n_{\mathrm{dry}}(z)}\frac{M_{\mathrm{H}}}{M_{\mathrm{dry}}} \tag{3}$$

where $n_{\mathrm{dry}}(z)$ is the number density of dry air at height z. M_{H} and M_{dry} refer to the water vapor and dry air molecular weight respectively. Nitrogen is in constant (about 78%) proportion to dry air at the heights over which these measurements were made, and thus the Raman nitrogen return signal is used as a measure of the mass of dry air.

$$w(z)=\frac{n_{\mathrm{H}}(z)}{n_{\mathrm{N}}(z)}\frac{M_{\mathrm{H}}}{M_{\mathrm{dry}}}\frac{n_{\mathrm{N}}(z)}{n_{\mathrm{dry}}(z)} \tag{4}$$

The mixing ratio then can be determined from the lidar data by using the Raman-shifted signals from water vapor and nitrogen. By using Eqs. (1) and (2), the mixing ratio $w(z)$ can be expressed as

$$w(z)=C_{\mathrm{H}}\Delta_q^{\mathrm{H}}(z_0,z)\frac{S_{\mathrm{H}}(z)}{S_{\mathrm{N}}(z)} \tag{5}$$

where

$$C_{\mathrm{H}} = \frac{k_{\mathrm{N}}}{k_{\mathrm{H}}} \frac{\sigma_{\mathrm{N}}(\pi)}{\sigma_{\mathrm{H}}(\pi)} \frac{M_{\mathrm{H}}}{M_{\mathrm{dry}}} \frac{n_{\mathrm{N}}(z)}{n_{\mathrm{dry}}(z)} \tag{6}$$

is the system calibration constant for the water vapor mixing ratio measurement and

$$\Delta_q^{\mathrm{H}}(z_0, z) = \frac{q(\lambda_{\mathrm{N}}, z_0, z)}{q(\lambda_{\mathrm{H}}, z_0, z)} \tag{7}$$

is the transmission correction function for the water vapor mixing ratio calculation. From Eq. (5), the mixing ratio is seen to be proportional to the ratio of Raman lidar signals for water vapor and nitrogen with the exception of the transmission correction term $\Delta_q^{\mathrm{H}}(z_0, z)$.

With the influence of each overlap factor, the signals of "short range" in Raman water vapor channel and Raman nitrogen channel need to be calibrated with channel correcting factor. The corrected signal ratio of water vapor and nitrogen can be expressed as

$$\frac{S_{\mathrm{H}}(z)}{S_{\mathrm{N}}(z)} = \frac{S'_{\mathrm{H}}(z)/\gamma_{\mathrm{H}}(z)}{S'_{\mathrm{N}}(z)/\gamma_{\mathrm{N}}(z)} = \frac{S'_{\mathrm{H}}(z)}{S'_{\mathrm{N}}(z)} \cdot \frac{\gamma_{\mathrm{N}}(z)}{\gamma_{\mathrm{H}}(z)} \tag{8}$$

where $s_x(z)$ is the corrected return signal in channel x; $s'_x(z)$ is the measured return signal in channel x; $\gamma_x(z)$ is the overlap factor in channel x.

From Eq. (8), we find that the ratio of water vapor signal and nitrogen signal can be calibrated by the ratio of each overlap factor in two channels $\gamma_{\mathrm{H}}(z)/\gamma_{\mathrm{N}}(z)$, and the exact value of every overlap factor need not be known. The channel correcting factor is measured from the return lights at the same nitrogen Raman-shifted wavelength of 386.7 nm in two channels. The ratio of nitrogen Raman scattered signals in two channels is presented in Eq. (9).

$$\frac{S_{2\mathrm{N}}(z)}{S_{1\mathrm{N}}(z)} = \frac{K_{\mathrm{N}}}{K_{\mathrm{H}}} \cdot \frac{\gamma_{\mathrm{N}}(z)}{\gamma_{\mathrm{H}}(z)} = K \cdot \frac{\gamma_{\mathrm{N}}(z)}{\gamma_{\mathrm{H}}(z)} \tag{9}$$

Here, k_x is the constant of lidar system in channel x, and k is the ratio between them. Because the signals are not affected by the overlap factors over large ranges such as 1.5 km, the ratio $\gamma_{\mathrm{H}}(z)/\gamma_{\mathrm{N}}(z)$, will be equal to the unity. In such a condition, $\lambda_{\mathrm{H}}(1.5)/\gamma_{\mathrm{N}}(1.5) = 1$, and $k = S_{2\mathrm{N}}(1.5)/S_{1\mathrm{N}}(1.5)$ can be obtained. So the channel correcting factor can be calculated in the following equation.

$$\frac{\gamma_{\mathrm{N}}(z)}{\gamma_{\mathrm{H}}(z)} = \frac{S_{2\mathrm{N}}(z)}{S_{1\mathrm{N}}(z)} \left[\frac{S_{2\mathrm{N}}(1.5)}{S_{1\mathrm{N}}(1.5)} \right]^{-1} \tag{10}$$

Finally, by using Eqs. (10) and (8), the correction of signals in "short range" is done.

The transmission correction function can be calculated from the aerosol and molecular extinctions at the water and nitrogen Raman-shifted wavelengths. In the present experiment using RML lidar, the aerosol extinction coefficient is derived from the measured aerosol extinction coefficient at 532 nm with a λ^{-1} wavelength dependence. And the molecular extinctions at two wavelengths are obtained from the data of standard atmospheric model with a λ^{-4} wavelength dependence in the wavelength range of the experiment (386.7–532 nm). Once the transmission correction function is accounted for, the constant C_{H} is determined by calibration with respect to a simultaneous radiosonde.

4 Observation examples

Using RML lidar, measurement of water vapor was taken during night or day without low cloud, and consisted of three steps. In the first step, 30 000 shots of laser were emitted, and the return signals over "long range" (>1–2 km) were detected in two channels with active gate circuit of PMT. The second step is similar to the first one with the exception of the inactive gate circuit of PMT, and the signals at "short range" (<3 km) were observed. In the last step, the interference filter of 407.8 nm in water vapor Raman channel was replaced by the filter of 386.7 nm and the corresponding attenuations were added. The same nitrogen Raman scattered signals were measured in both channels for obtaining the channel correcting factor, which is used to calibrate the difference between signals caused by the dissimilar overlap factors. The whole experiment took about one hour, and the resolution of range was 30 m.

4.1 Water vapor mixing ratio observed at night

Figure 2 gives two typical results (solid line) of water vapor mixing ratio obtained by RML lidar over Hefei, at about 21:00 on Sep. 12 and Oct. 9 2004, respectively. For comparison, the simultaneously measured profiles of water vapor by L625 lidar (dot line) and the GZZ-59 type radiosonde (square line) with reference to relative humidity RH = 20% (short dot line) are also shown in Fig. 2. L625 lidar is the multipurpose lidar developed by AIOFM, and the measurements of water vapor were taken in 1999. Because of its own limitations, the L625 lidar just observed the water vapor over a height of 1 km at night.

It is found from Fig. 2 that the RML lidar measured data agreed well with the data obtained by L625 lidar in the same range of 1 km and 5.5 km, and the relative differences were less than 20%. The agreement of the observation between RML lidar data and radiosonde data was also present in most of the measured ranges, and some discrepancies appeared in conditions such as when the content of water vapor was lower or it changed violently with height. Three factors may probably produce these differences. One is that the GZZ-59 radiosonde has larger measuring errors in lower air moisture (relative humidity $<20\%$) and when the change of moisture is very fast, especially from the higher moisture to the lower one. Systematic biases of GZZ-59 radiosonde are usually 5%–10% under the mid-height moisture conditions, or even worse at the temperature below 0°C, when compared with

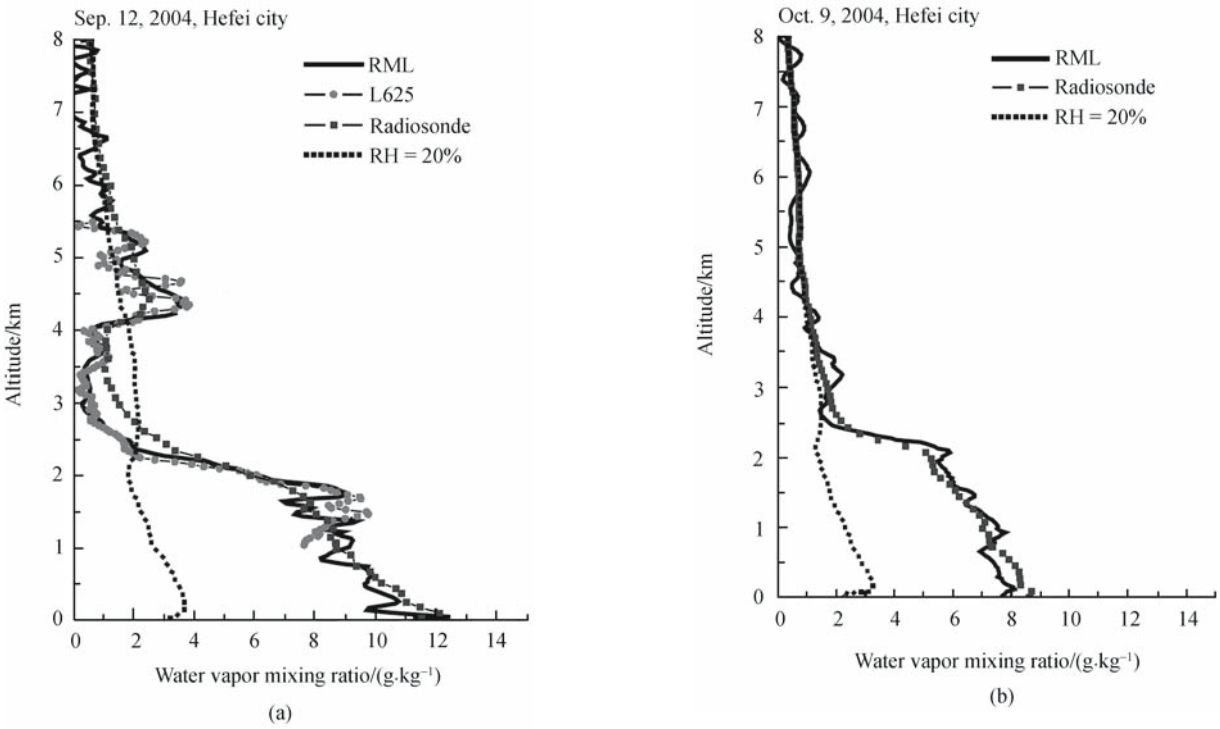

Fig. 2 Profiles of water vapor during the nights of Sep. 12 and Oct. 9 2004, Hefei

RS-80 and VIZ-1392 radiosondes. Intercomparisons of water vapor profiles by other Raman lidars and radiosondes also demonstrate this situation. Therefore, higher accuracy humidity sensor of radiosonde is greatly expected for calibrating Raman lidar data for water vapor measurement. The other is the differences in measuring time and ambient air by Raman lidar and radiosonde. Usually, lidar gives the one-hour mean of water vapor distribution in the vertical point of lidar, but GZZ-59 radiosonde obtains the transient humidity at some altitudes on its ascending pathways. The third factor is in association with the measured capability of RML lidar for lower content of water vapor. When the number of water vapor molecule in air is less, the Raman return signals scattered by them are thin, and thus the measured errors of RML lidar become greater.

From comparing profiles of water vapor mixing ratio measured on these two days, we can find that both of them show a boundary layer where the water vapor mixing ratio decreases greatly with respect to the height. Most of the water vapor existing below this layer and the mixing ratio usually was not greater than 2 g/kg over this layer. The height of this layer differed with days, and it ranged from about 1.5 km to 3 km in normal conditions. The difference between results as shown in Figs. 2(a) and (b) shows that some layers of water vapor appeared in the range of 1–4.5 km on Sep. 12, but it disappeared on Oct. 9. This reveals the complexity of the water vapor's temporal and spatial distribution in atmosphere.

The observed results as explained above not only show that the measurement of water vapor by RML lidar is right and reliable, but also indicates that this lidar has the ability to observe the characteristics of water vapor from near surface up to about 7–8 km height at night.

4.2 Water vapor mixing ratio in cloud

Because cloud effect is one of the most uncertain parts of climatic prediction, and the net effect depends on the types of cloud and their optical properties and so on, the measurement of water vapor mixing ratio appears very important and necessary in understanding these effects. Figure 3(b) gives the example of water vapor mixing ratio in cloud observed on Oct. 27 2004, and the simultaneous aerosol extinction (a) is also shown in the figure. In natural conditions, both aerosol extinction and water vapor mixing ratio decrease with the elevation. However, with the influence of clouds, either aerosol extinction or water vapor mixing ratio enlarged in ranges of 1–1.5 km, 2–3.5 km and 4–5 km on this day. The biggest extinction is greater than 0.5 km^{-1} in the lowest cloud, and the corresponding mixing ratio was up to 6.2 g/kg. The consistency of the two measured profiles shows that there existed a strong relationship between water vapor and aerosols. This result also demonstrated that RML lidar system is a valuable tool in studying how changes in water vapor affect the optical and physical characteristics of aerosols because these changes can be observed remotely throughout a large depth of the atmosphere.

4.3 Water vapor mixing ratio measured in daytime

Observation in daytime is always a challenge to lidar system because of the effects from the violent solar background

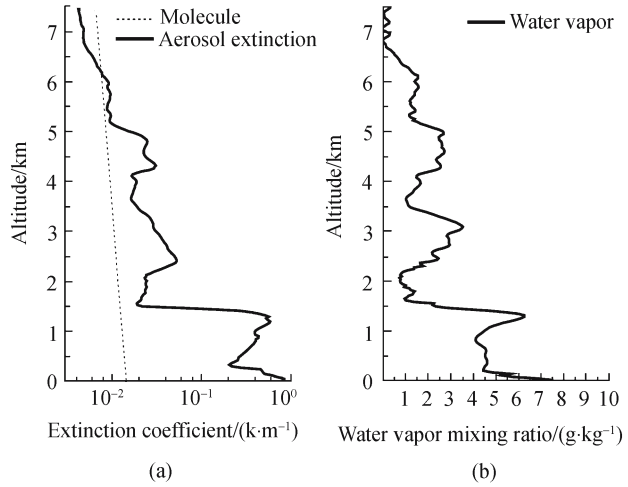

Fig. 3 Profiles of aerosol extinction and water vapor mixing ratio on a cloudy day
(a) Extinction coefficient; (b) Water vapor mixing ratio

radiation. One of the targets of this study was to try and gain experience in improving the ability of lidar's measurement during daytime. Although some techniques were taken in design, RML lidar is still not suitable to observe the water vapor at noon, but measure it in boundary layer at sunrise or sunset when the background radiation was not so high. An example of measurement by RML lidar at sunset (solid line) is given in Fig. 4, and the observation at night (dot line) is also presented together. From the Figure, it can be seen that a distinct boundary layer was presented at a height about 1 km on this day, and the structure of water vapor was stable from sundown to night. Over the boundary layer, the profile of water vapor during daytime appeared to have greater vibrancy because of disturbance by the strong solar background radiation. Results of experiments conducted during daytime indicated that RML lidar had a limited ability to observe

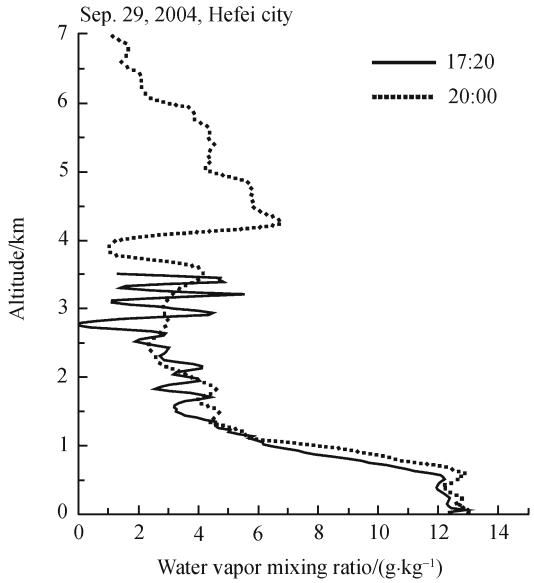

Fig. 4 Profile of water vapor measured by RML lidar in daytime

the water vapor during daytime, but there was more room to improve. For advancing the ability to observe water vapor in daytime, some modifications such as the increase of laser energy and frequency, reduction of the field of view and the passbands of the Raman filters, will be applied in RML lidar system in the next research.

5 Conclusions

The first mobile Raman lidar system (RML lidar) was developed at AIOFM and is introduced in this paper. This lidar is used to observe the tropospheric water vapor during daytime and at night. Some comparisons of experimental examples with L625 lidar and radiosonde are presented in this paper. Experimental results demonstrate that the RML lidar system is a powerful tool for direct observation of tropospheric water vapor during daytime and at night. Under night conditions, the observations cover a range from near surface up to the height of 8 km, whereas, daytime limits the observations to the boundary layer, which is dependent on water vapor content of the atmosphere.

Acknowledgements This work was supported by the Hi-Tech Research and Development Program of China.

References

1. Zhou Xiuji, Tao Shanchang, Yao Keya. Advanced Atmospheric Physics. Beijing: Meteorological Press, 1990 (in Chinese)
2. Shine K P, Sinha A. Sensitivity of the Earth's climate to height-dependent changes in the water vapor mixing ratio. Nature, 1991, 354: 382–384
3. Yan Fengqi, Hu Huanling, Zhou Jun. Measurements of number density distribution and imaginary part of refractive index of aerosol particles. Acta Optica Sinica, 2003, 23(7): 855–859 (in Chinese)
4. Zhou Bin, Liu Wenqing, Qi Feng, et al. Error analysis in differential optical absorption spectroscopy. Acta Optica Sinica, 2002, 22(8): 957–961 (in Chinese)
5. Hu Huanling, Wu Yonghua, Xie Chenbo. Aerosol pollutant boundary layer measured by lidar at Beijing. Research of Environmental Sciences, 2004, 17(1): 59–66 (in Chinese)
6. Liu Dong, Qi Fudi, Jin Chuanjia. Polarization lidar observations of cirrus clouds and Asian dust aerosols over Hefei. Chinese Journal of Atmospheric Sciences, 2003, 27(6): 1 093–1 100 (in Chinese)
7. Hu Shunxing, Hu Huanling, Wu Yonghua, et al. L625 Differential absorption lidar system for tropospheric ozone measurements. Acta Optica Sinica, 2004, 24(5): 597–601 (in Chinese)
8. Zhang Yinchao, Hu Huanling, Tan Kun, et al. Development of a mobile lidar system for air pollution monitoring. Acta Optica Sinica, 2004, 24(8): 1 025–1 031 (in Chinese)
9. Wu Yonghua, Hu Huanling, Hu Shunxing, et al. Rayleigh-Raman scattering lidar for atmospheric temperature profiles measurements. Chinese Journal of Lasers, 2004, 31(7): 851–856 (in Chinese)
10. Melfi S H, Lawrence J D, McCormick M P. Observation of Raman scattering by water vapor in the atmosphere. Appl Phys Lett, 1969, 15: 295–297

11. Cooney J A. Remote measurements of atmospheric water vapor profiles using the Raman component of laser backscatter. J Appl Meteorol, 1970, 9: 182–184
12. Melfi S H, Whiteman D N, Ferrare R A. Observations of atmospheric fronts using Raman lidar moisture measurements. J Appl Meterol, 1989, 28: 789–806
13. Ansman A, Riebesell M, Wandinger U, et al. Combined Raman elastic-backscatter lidar for vertical profiling of moisture, aerosol extinction, backscatter, and lidar ratio. Appl Phys, 1992, 55: 18–28
14. Whiteman D N, Melfi S H, Ferrare R A. Raman lidar system for the measurement of water vapor and aerosols in the Earth's atmosphere. Appl Opt, 1992, 31: 3 068–3 082
15. Xie Chenbo, Han Yong, Li Chao, et al. Mobile lidar for visibility measurement. High Power Laser and Particle Beams, 2005, 17(7): 971–975 (in Chinese)